An adaptative antidissipative method for optimal control problems

Olivier Bokanowski, Nadia Megdich, Hasnaa Zidani

INRIA

INSTITUT NATIONAL DE RECHERCHE EN INFORMATIQUE ET EN AUTOMATIQUE

An adaptative antidissipative method for optimal control problems

Olivier Bokanowski — Nadia Megdich — Hasnaa Zidani

N° 5770

Novembre 2005

Thème NUM

ISSN 0249-6399 ISRN INRIA/RR--5770--FR+ENG

INRIA
ROCQUENCOURT

An adaptative antidissipative method for optimal control problems

Olivier Bokanowski* , Nadia Megdich† , Hasnaa Zidani‡

Thème NUM — Systèmes numériques
Projet SYDOCO

Rapport de recherche n° 5770 — Novembre 2005 — 21 pages

Abstract: We deal with a numerical method for HJB equations coming from optimal control problems with state constraints.
More precisely, we present here an antidissipative scheme applied on an adaptative grid.The adaptative grid is generated using linear quadtree structure. This technique of adaptation facilitates stocking data and dealing with large numerical systems.

Key-words: optimal control problems, HJB equations, antidissipative scheme, linear quadtree.

* Lab. Jacques-Louis Lions, Université Pierre et Marie Curie, 175 Rue Chevaleret 75013 Paris, France. Email: boka@math.jussieu.fr
† ENSTA, UMA, 32 Boulevard Victor, 75739 Paris Cedex 15, France. Also at Projet SYDOCO, INRIA Rocquencourt, BP 105, 78153 Le Chesnay. Emails: Nadia.Megdich@ensta.fr.
‡ ENSTA, UMA, 32 Boulevard Victor, 75739 Paris Cedex 15, France. Also at Projet SYDOCO, INRIA Rocquencourt, BP 105, 78153 Le Chesnay. Emails: Hasnaa.Zidani@ensta.fr.

Unité de recherche INRIA Rocquencourt
Domaine de Voluceau, Rocquencourt, BP 105, 78153 Le Chesnay Cedex (France)
Téléphone : +33 1 39 63 55 11 —Télécopie : +33 1 39 63 53 30

An adaptative antidissipative method for optimal control problems

Résumé : On étudie une méthode numérique pour les équations HJB provenant des problèmes de contrôle optimal avec contraintes sur l'état. Plus précisèment on présente un schéma antidissipatif sur une grille adaptative. La grille adaptative est générée en utilisant la structure des quadtree linéaires. Cette technique facilite le stockage et la maniabilité des mailles.

Mots-clés : problèmes de contrôle optimal, équations HJB, schéma antidissipatif, quadtree linéaire.

1 Introduction

In this paper, we deal with an optimal control problem $(\mathcal{P}_{s,x})$ with state constraint:

$$\left\{\begin{array}{l} \min \varphi(y_{x,s}(T)), \\ \dot{y}_{x,s}(t) = f(y_{x,s}(t), a(t)) \ \forall t \in [s,T] \\ y_{x,s}(s) = x, \ x \in \boldsymbol{R}^n, \\ a(t) \in \mathcal{A} \text{ a.e } , \ \forall t \in [s,T], \\ y_{x,s}(t) \in \mathcal{K} \ \ \forall t \in [s,T]. \end{array}\right. \tag{1}$$

The set of controls $\mathcal{A}$ is a compact of $\boldsymbol{R}^m$, $\varphi : \boldsymbol{R}^n \to \boldsymbol{R} \cup \{+\infty\}$ is lower semi continuous (l.s.c) and T is a fixed final time. The set $\mathcal{K} \neq \emptyset$ is a compact convex set of $\boldsymbol{R}^n$. The dynamics $f : \boldsymbol{R}^n \times \mathcal{A} \to \boldsymbol{R}^n$ is assumed to be Lipschitz and bounded.

Let $v : [0,T] \times \boldsymbol{R}^n \to \boldsymbol{R} \cup \{+\infty\}$ be the value function defined by $v(s,x) = \inf(\mathcal{P}_{s,x})$. For every $s \in [0,T]$ and $x \notin \mathcal{K}$, $v(s,x) = +\infty$ and for $x \in \mathcal{K}$, $v(T,x) = \varphi(x)$.
It is known that the value function v satisfies the *Dynamic Programming Principle* (DPP):

$$v(s,x) = \inf_{a(.) \in A(s,\tau;x)} v(\tau, y_{x,s}(\tau)), \qquad \forall \tau \in]s,T], \ \forall x \in \mathcal{K}, \tag{2}$$

where $A(s,\tau;x) := \{a : [0,+\infty[\to \mathcal{A} \text{ measurable}, \ y_{x,s}(t) \in \mathcal{K}, \ \forall t \in [s,\tau]\}$.

In the case when the final cost function φ is continuous and $\mathcal{K} = \boldsymbol{R}^n$, the value function is the unique continuous "viscosity" solution [1, 2, 8] of the *Hamilton-Jacobi-Bellman* (HJB) equation:

$$\left\{\begin{array}{ll} -v_t(t,x) - \min_{a \in \mathcal{A}} f(x,a).v_x(t,x) = 0, & (t,x) \in [0,T] \times \mathcal{K}, \\ v(T,x) = \varphi(x), & x \in \mathcal{K}. \end{array}\right. \tag{3}$$

In this paper, we are interested in the case when φ is given by

$$\varphi(x) = \left\{\begin{array}{ll} 0 & \text{if } x \in \mathcal{C}, \\ +\infty & \text{otherwise,} \end{array}\right. \tag{4}$$

where $\mathcal{C} \neq \emptyset$ is a compact convex set of $\boldsymbol{R}^n$, $\mathcal{C} \subset \mathcal{K}$ and $\mathcal{K} \neq \boldsymbol{R}^n$. In section 4, we will see that this case modelizes several control problems (target problem, Rendez-Vous problem, viability kernels,...). Here, the value function v may clearly be discontinuous and takes its values in $\{0, +\infty\}$. It still satisfies equation (3) in a sense given by Frankowska and her co-authors [16, 17]. For more details about the different notions of solution of the HJB equation, see the appendix and the references therein.

Several numerical schemes have been studied for discretizing (3). The most popular are the Semi-Lagrangian schemes [12, 13, 19] and the finite differences schemes [22, 9]. These schemes provide a good approximation for a continuous value function. However, they all use interpolation techniques at some level and are no more suitable for the approximation of discontinuous value functions. Indeed, the interpolation steps produce more or less numerical diffusion, which causes an increasing loss of precision mainly around the discontinuities.
To our knowledge, the only scheme which doesn't use any interpolation technique is the one

based on the viability algorithm developed by P. Saint Pierre and his co-authors [21]. But, as already shown in [6] this scheme still diffuses.

The approximation method we study here is a mixture of the antidissipative *UltraBee* (UB) scheme [11, 5] and of an adaptative gridding technique. The UltraBee scheme has been studied by B. Després and F. Lagoutière [11] for solving the transport equation with positive constant velocity. It has been extended by O. Bokanowski and H. Zidani [5] for the transport equation with a changing sign velocity and applied for the resolution of Hamilton Jacobi equations (3) on a regular grid.
In our case, the value function takes only values 0 and 1 (the value 1 coding in fact the $+\infty$ value). In this special situation, the UltraBee scheme has a nice property: it is able to localize accurately the discontinuity of v corresponding to the interface Γ_t separating the region where $v(t,.)$ takes the value 1 from the region where it takes the value 0. This property allows us to design a simple method for adaptative gridding. Moreover, the real calculations at every time $t^n = n\Delta t$ (Δt being the time step) have only to be done on a small neighborhood of the interface Γ_{t^n}. Hence adaptative gridding is particularly interesting in our case. Moreover, we use linear quadtrees which provide a good way to handle easily adaptative grids and to achieve a significant save of memory.

Adaptative gridding for solving HJB equations has already been studied in the case of a continuous value function. In [19], L.Grune has handled the Semi-Lagrangian scheme to solve (3) and explained the criteria he used for the refinement and coarsening steps. These criteria are based on a fixed tolerance for the interpolation error. The presence of discontinuities in our case makes these criteria no more suitable.

The paper is organized as follows. In section 2 we give the formulation of the UltraBee scheme and some of its properties. In section 3 we present the adaptative technique that we use and explain the steps of the proposed method. Finally in section 4, we give several numerical simulations in 2 dimensions coming from control problems and propagating front problems.

2 The UltraBee scheme

Notice that when we deal with only one control, the HJB equation (3) becomes a transport equation. Hence we will first present the UltraBee scheme in this simple case in one space dimension ($n = 1$).

2.1 Transport equation

Let $f : \boldsymbol{R} \to \boldsymbol{R}$ be Lipschitz and bounded and $u_0 : \boldsymbol{R} \to \boldsymbol{R}$ be lower semi continuous. We consider the transport problem:

$$\begin{cases} u_t(t,x) + f(x)u_x(t,x) = 0, \ x \in \boldsymbol{R}, \ t \geq 0, \\ u(0,x) = u_0(x), \ x \in \boldsymbol{R}. \end{cases} \tag{5}$$

In all the sequel, we will use the following notations: Δt denotes the time step, Δx is the space step of a regular grid $\mathcal{G}$ of $\boldsymbol{R}$ and ν_j is the local CFL number at cell M_j defined by:

$$\nu_j := \frac{f(x_j)\Delta t}{\Delta x}.$$

Consider the following scheme of finite volumes type:

$$\begin{cases} \dfrac{U_j^{n+1} - U_j^n}{\Delta t} + f(x_j)\dfrac{U_{j+\frac{1}{2}}^{n,L} - U_{j-\frac{1}{2}}^{n,R}}{\Delta x} = 0, \ \forall j \in \mathbb{Z}, \ \forall n \in \mathbb{N}, \\ U_j^0 = \dfrac{1}{\Delta x}\displaystyle\int_{M_j} u_0(x)dx, \ \forall j \in \mathbb{Z}. \end{cases} \tag{6}$$

where x_j is the middle point of cell $M_j = [x_{j-\frac{1}{2}}, x_{j+\frac{1}{2}}]$, U_j^n is an approximation of the mean value $\dfrac{1}{\Delta x}\displaystyle\int_{M_j} u(t^n, x)dx$ of u on cell M_j at t^n, and $U_{j+\frac{1}{2}}^{n,L}$, $U_{j+\frac{1}{2}}^{n,R}$ are fluxes respectively on the left and on the right of the interface of cells M_j and M_{j+1} at time t^n.
For the UltraBee scheme, these fluxes are defined in the following way.

- In the case when the velocity $f(.) \equiv f$ is a positive constant, the fluxes $U_{j+\frac{1}{2}}^{n,L}$ and $U_{j+\frac{1}{2}}^{n,R}$ coincide and we have $U_{j+\frac{1}{2}}^{n,L} = U_{j+\frac{1}{2}}^{n,R} =: U_{j+\frac{1}{2}}^n$. The scheme becomes:

$$\frac{U_j^{n+1} - U_j^n}{\Delta t} + f(x_j)\frac{U_{j+\frac{1}{2}}^n - U_{j-\frac{1}{2}}^n}{\Delta x} = 0.$$

  The UltraBee scheme, as defined in [11], is a downwind choice of the fluxes under some stability conditions. This choice replaces the classical Upwind flux which is stable but dissipative. More precisely, the flux $U_{j+\frac{1}{2}}^n$ is given by solving the minimization problem: $\min_{b_j^{n,+} \le U \le B_j^{n,+}} |U - U_{j+1}^n|$ where $b_j^{n,+}$ and $B_j^{n,+}$ are defined by:

$$b_j^{n,+} = \frac{1}{\nu_j}(U_j^n - \max(U_j^n, U_{j-1}^n)) + \max(U_j^n, U_{j-1}^n),$$

$$B_j^{n,+} = \frac{1}{\nu_j}(U_j^n - \min(U_j^n, U_{j-1}^n)) + \min(U_j^n, U_{j-1}^n).$$

  It follows that

$$U_{j+\frac{1}{2}}^n = \min(\max(U_{j+1}^n, b_j^{n,+}), B_j^{n,+}). \tag{7}$$

- In the case when f is of changing sign, the *UltraBee generalized scheme* (UB-G) [5] is defined as follows

  (a) if $\nu_j > 0$, $U_{j+\frac{1}{2}}^{n,L} = \min(\max(U_{j+1}^n, b_j^{n,+}), B_j^{n,+})$ as proposed in (7).

(b) if $\nu_j < 0$, we define symetrically $U^{n,R}_{j-\frac{1}{2}} = \min(\max(U^n_{j-1}, b^{n,-}_j), B^{n,-}_j)$ with
$b^{n,-}_j = \frac{1}{|\nu_j|}(U^n_j - \max(U^n_j, U^n_{j+1})) + \max(U^n_j, U^n_{j+1})$, and
$B^{n,-}_j = \frac{1}{|\nu_j|}(U^n_j - \min(U^n_j, U^n_{j+1})) + \min(U^n_j, U^n_{j+1})$.

(c) if $\nu_j \leq 0$ and $\nu_{j+1} \geq 0$, $U^{n,L}_{j+\frac{1}{2}} = U^n_j$, $U^{n,R}_{j+\frac{1}{2}} = U^n_{j+1}$.

(d) if $\nu_j\nu_{j+1} > 0$, $U^{n,R}_{j+\frac{1}{2}} = U^{n,L}_{j+\frac{1}{2}}$ (if $\nu_j > 0$) or $U^{n,L}_{j+\frac{1}{2}} = U^{n,R}_{j+\frac{1}{2}}$ (if $\nu_{j+1} < 0$).

When the velocity is constant, and under the CFL condition,

$$|\nu_j| \leq 1 \ \forall j \in \mathbb{Z}, \tag{8}$$

one interesting property of the UltraBee scheme is an exact advection [11, Theorem 3] for a class of step functions defined by: $\exists k^0 \in [0,1[$ such that $\forall j \in \mathbb{Z}$,

$$U^0_{3j+1} = U^0_{3j}, \quad U^0_{3j+2} = k^0 U^0_{3j+1} + (1-k^0)U^0_{3j+3}. \tag{9}$$

Exact advection means that the computed value U^n_j is the exact mean value,

$$U^n_j = \frac{1}{\Delta x}\int_{M_j} u(t^n, x)dx,$$

where u is the exact solution of the advection problem. For the convergence proofs of the UltraBee scheme, we refer to [11, 5].

Now using the splitting technique, we define the UB scheme for 2D problems. Let $\mathcal{G}$ be a regular grid in $\mathbb{R}^2$. We denote by $M_{j,k}$ a cell of $\mathcal{G}$ with center (x^1_j, x^2_k) and mesh size $(\Delta x^1, \Delta x^2)$, the velocity $f = (f_1, f_2)$. We explain in the following the Trotter splitting technique which consists in evolving during a step of time in the x^1-direction and then during another step of time in the x^2-direction:

$$\begin{cases} \dfrac{U^{n+1,1}_{j,k} - U^n_{j,k}}{\Delta t} + f_1(x^1_j, x^2_k)\dfrac{U^{n,L}_{j+\frac{1}{2},k} - U^{n,R}_{j-\frac{1}{2},k}}{\Delta x^1} = 0, \ \forall j,k \in \mathbb{Z}, \ \forall n \in \mathbb{N}, \\ \dfrac{U^{n+1}_{j,k} - U^{n+1,1}_{j,k}}{\Delta t} + f_2(x^1_j, x^2_k)\dfrac{U^{n,L}_{j,k+\frac{1}{2}} - U^{n,R}_{j,k-\frac{1}{2}}}{\Delta x^2} = 0, \ \forall j,k \in \mathbb{Z}, \ \forall n \in \mathbb{N}, \\ U^0_{j,k} = \dfrac{1}{\Delta x^1 \Delta x^2}\displaystyle\int_{M_{j,k}} u_0(x^1, x^2)dx^1dx^2, \ \forall j,k \in \mathbb{Z}. \end{cases} \tag{10}$$

Here the fluxes $(U^{n,L}_{j+\frac{1}{2},k})_j$ and $(U^{n,R}_{j-\frac{1}{2},k})_j$ are respectively the left and right UB-G fluxes defined using the $(U^n_{j,k})_{j\in\mathbb{Z}}$ with an evolution only in the x^1-direction with velocity f_1. The fluxes $(U^{n,L}_{j,k+\frac{1}{2}})_k$ and $(U^{n,R}_{j,k-\frac{1}{2}})_k$ are the UB-G fluxes defined using the $(U^{n+1,1}_{j,k})_{k\in\mathbb{Z}}$ with an evolution occuring only in the x^2-direction with velocity f_2.
The resolution using this splitting technique is stable under the CFL condition,

$$\max(|\frac{f_1(x^1_j, x^2_k)\Delta t}{\Delta x^1}|, |\frac{f_2(x^1_j, x^2_k)\Delta t}{\Delta x^2}|) \leq 1, \ \forall (j,k) \in \mathbb{Z}^2. \tag{11}$$

2.2 HJB equation

Here, we are still in dimension 1. First, we consider the simple change of variable,

$$\hat{v}(t,x) = v(T-t,x),\ \forall t \in [0,T],\ \forall x \in \boldsymbol{R}.$$

Then the function $\hat{v}$ satisfies

$$\begin{cases} \hat{v}_t(t,x) - \min\limits_{a\in\mathcal{A}} f(x,a).\hat{v}_x(t,x) = 0,\ \forall (t,x) \in [0,T]\times\mathcal{K}, \\ \hat{v}(0,x) = \varphi(x),\ \forall x \in \mathcal{K}. \end{cases} \tag{12}$$

The application of UB-G to the HJB equation (12) consists, on a regular grid $\mathcal{G}$ of $\mathcal{K}$, in the following steps (UB-HJB):

- Step 1: We compute the discrete initial condition

$$V_j^0 = \frac{1}{\Delta x}\int_{M_j} \varphi(x)dx,\ \forall j \in J := \{j \in \mathbb{Z},\ M_j \in \mathcal{G}\}.$$

- Step 2: We discretize the set of controls $\mathcal{A}$ into N_a controls, $a_1, a_2, ..., a_{N_a}$.
- Step 3: For $n \geq 1$, knowing the approximation $(V_j^n)_{j\in J}$ of $\hat{v}(t^n,.)$
  - We compute, for each $i = 1...N_a$, $(U_j^{n+1}(a_i))_{j\in J}$ given by the UB-G scheme:

$$\begin{cases} U_j^{n+1}(a_i) = U_j^n(a_i) - \dfrac{f(x_j,a_i)\Delta t}{\Delta x}(U_{j+\frac{1}{2}}^{n,L}(a_i) - U_{j-\frac{1}{2}}^{n,R}(a_i)), \\ U_j^n(a_i) = V_j^n, \quad \forall j \in J. \end{cases}$$

  - We take $V_j^{n+1} := \min\limits_{i=1..N_a} U_j^{n+1}(a_i),\ \forall j \in J$. This defines the numerical approximation of $\hat{v}$ at t^{n+1}.

Notice that the CFL condition must be satisfied for each control,

$$\left|\frac{f(x_j,a_i)\Delta t}{\Delta x}\right| \leq 1,\ \forall j \in J,\ \forall i = 1,..,N_a.$$

In [7], under some suitable assumptions, we prove in one space dimension the convergence of the UB-HJB scheme towards the value function for any initial condition φ which is C^1-piecewise regular with compact support.

Notice that, at the first step of UB-HJB scheme, when we compute the average values $(V_j^0)_{j\in J}$, the only components whose values are strictly between 0 and 1 are those correponding to the cells containing the front Γ_0 (we recall that Γ_0 is the interface separating 0-values of $\hat{v}(t=0,.)$ and its 1-values).

In dimension 1, we prove in [7] that, for every $n \geq 0$, the interface Γ_{t^n} is localized on no more than one cell. In dimension 2, we shall verify numerically that Γ_{t^n} is still well localized by the UB-HJB scheme, but we don't have yet any precise theoretical result to claim.

3 The adaptative method

We explain in this section the details of the method that we propose. For sake of simplicity, we take $n = 2$ and $\mathcal{K} = [X^1_{\min}, X^1_{\max}] \times [X^2_{\min}, X^2_{\max}]$. Before dealing with details, we start by presenting the linear quadtrees technique that we use for stocking data.

3.1 Linear quadtrees

As we deal with adaptative grids, we look for a technique that facilitates stocking and finding data relative to each cell of the grid. This technique is explained by I. Gargantini in [18] and uses the notion of *linear quadtree*. If we represent our final adapted grid by a tree, each cell is a leaf (final node of the tree) and the initial quadrant (all the domain $\mathcal{K}$ before adaptation) is the root of the tree. The method for stocking data using quadtrees is based on coding each leaf of the tree with a quaternary function. This code representation is implicitly the path from the root to the concerned leaf.
Every code is composed of 0, 1, 2, 3. When dividing a cell into four subcells, the NW quadrant is indexed by 0, the NE by 1, the SW by 2 and the SE by 3. The code of each subcell is the concatenation of the code of the mother cell with the index of the subcell (as shown in figure 3.1). Here cells 20, 21, 22 and 23 are sisters and 2 is the mother cell.

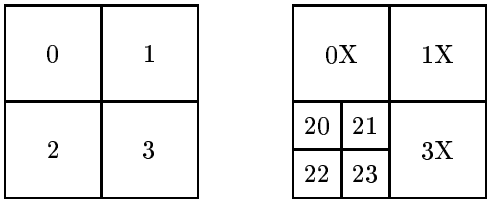

Figure 1: Refinement of a cell by quadtrees

Notice that when coding the grid using a tree, all intermediate cells have to be memorized, for example we memorize cells 2, 20, 21, 22, 23. However, in a linear quadtree, we have to stock only final cells of the grid, i.e. cells 20, 21, 22, 23. Then, to find the intermediate cells, we have just to truncate the codes. Furthermore the use of linear quadtrees allows to manage efficiently the adapted grid. In fact, thanks to fast algorithms, operations like encoding a cell into its quaternary code and finding adjacencies of a cell are run in logarithmic time [18].

3.2 Algorithm of the method

Our contribution consists in finding a suitable criterion to adapt the computational domain. This criterion must be compatible with the fact that we deal with mean values on each cell and that our value function is discontinuous.

Let $L_{\max}$ be a fixed integer that corresponds to the maximal level of refinement. We set $\Delta X^1_{\min} = \frac{|X^1_{\max} - X^1_{\min}|}{2^{L_{\max}}}$ and $\Delta X^2_{\min} = \frac{|X^2_{\max} - X^2_{\min}|}{2^{L_{\max}}}$. Then $(\Delta X^1_{\min}, \Delta X^2_{\min})$ is the minimal cell size. The maximal level $L_{\max}$ is chosen such that the following CFL condition holds:

$$\max(|\frac{f_1(x_j, a_i)\Delta t}{\Delta X^1_{\min}}|, |\frac{f_2(x_j, a_i)\Delta t}{\Delta X^2_{\min}}|) \leq 1, \ \forall j \in J, \ \forall i = 1, .., N_a. \tag{13}$$

In all the sequel, for every $n \geq 0$, we denote by $\mathcal{G}^n$ the adaptative grid at time $t_n = n\Delta t$. We also use the notation $\mathcal{G}_l$, $l = 1, \cdots, L_{\max}$, for the regular grid with mesh steps:

$$\Delta_l X^1 = \frac{|X^1_{\max} - X^1_{\min}|}{2^l}, \qquad \Delta_l X^2 = \frac{|X^2_{\max} - X^2_{\min}|}{2^l}.$$

We give now the algorithm of the method which begins by an initialization step. First, we handle refinement steps in order to localize the discontinuity. At every refinement level, a cell which is surrounded by cells not having the same mean value is refined. After these refinement steps, the grid we obtain may contain sister cells having the same mean value (0 or 1) as their immediate neighboring cells (a neighboring cell is a cell sharing an edge or a vertex with the concerned cell, it has not necessarily the same size). These cells do not contain any discontinuity and have to be coarsened: this is the coarsening steps. Finally, we get the grid $\mathcal{G}^0$ where a cell of minimal size either contains a discontinuity or is a neighbor of a cell containing a discontinuity or is a sister of such a cell.

Step 1: The construction of the grid $\mathcal{G}^0$.

- Step 1.1: Take $\mathcal{G}^{0,0} = \mathcal{K}$ (one cell), and define $\mathcal{G}^{0,1}$ as the domain $\mathcal{K}$ splitted into four cells. Set $l = 1$.
- Step 1.2: For $1 \leq l \leq L_{\max} - 1$. For all cells $M_j \in \mathcal{G}^{0,l} \setminus \mathcal{G}^{0,l-1}$, compare the value on M_j with its neighboring values. If the values are different, then refine cell M_j. We obtain a new grid denoted $\mathcal{G}^{0,l+1}$. Set $l = l + 1$ and go to Step 1.2.
  Otherwise, set $l = L_{\max}$ and go to Step 1.3.
- Step 1.3: Set $\widetilde{\mathcal{G}}^{0,L_{\max}} = \mathcal{G}^{0,L_{\max}}$.
- Step 1.4: For $l = L_{\max}, \cdots, 2$, for every cell $M_j \in \widetilde{\mathcal{G}}^{0,l} \cap \mathcal{G}_l$, if the sisters of M_j have the same mean value (0 or 1) and if the neighboring cells of the four sisters have also the same value, then coarsen M_j with its sisters. We obtain a new grid denoted $\widetilde{\mathcal{G}}^{0,l-1}$. Set $l = l - 1$, and go to Step 1.4. Otherwise, set $l = 1$, and go to Step 1.5.
- Step 1.5: Set $\mathcal{G}^0 := \widetilde{\mathcal{G}}^{0,1}$ and define V^0 on $\mathcal{G}^0$.

For example, the construction of the adapted grid $\mathcal{G}^0$ follows the refinement steps explicited in figure 3.2 for $L_{max} = 3$. The value function here takes value 1 below the discontinuity and value 0 beyond. At the second level of refinement, cell 2 is refined as its mean value is in $]0, 1[$. Cells 0, 1, 3 are refined too because their value 0 differs from the value of their

neighbor cell 2. Notice that, at level 3, $\mathcal{G}^{0,3}$ is such that all cells containing the discontinuity are of minimal size as well as their neighboring cells.
After refinement, we carry out a coarsening step. Following the test of the algorithm, we coarsen subcells of 21, 30, 32 and then subcells of 0, 1 and 3.

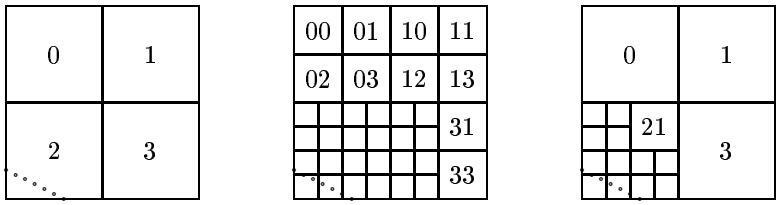

$\mathcal{G}^{0,1}$ $\mathcal{G}^{0,3}$ $\mathcal{G}^{0}$

Figure 2: Construction of $\mathcal{G}^0$, the discontinuity is plotted with dots.

Now, for $n \geq 0$, we have the adapted grid $\mathcal{G}^n$ (at time t^n) and the numerical solution V^n on $\mathcal{G}^n$. The discontinuity at t^n lies in the region of $\mathcal{G}^n$ where the cells are of minimal size. Because of the CFL condition (13), we know that the discontinuity is still in this region at t^{n+1} (as already explained the discontinuity does not evolve of more than one cell of size $(\Delta X^1_{\min}, \Delta X^2_{\min})$ during a time step). We conclude that $V_j^{n+1} = V_j^n$ (=0 or 1) whenever $M_j \in \mathcal{G}^n$ is not of minimal size, and the only computations which remain to be done correspond to the cells of minimal size $(\Delta X^1_{\min}, \Delta X^2_{\min})$. These calculations will be done with the UB-HJB scheme.

As we need neighboring values to do calculations on a given cell M_j of $\mathcal{G}^n$, one may wonder what is to be done for cells of minimal size with neighbors not of the same size. For example what to do for cell 21 in figure 3.1. In fact as a coarse cell is not of minimal size, we conclude that the function v takes everywhere 0 (or 1) on this cell. Hence, the mean value on the cell is 0 (or 1) and doesn't depend on the cell size: we use the mean value on the cell and do calculations as if it was of minimal size.

Step 2: UB-HJB computation and construction of $\mathcal{G}^{n+1}$.

- Step 2.0: Do an iteration of UB-HJB scheme on the cells of minimal size $(\Delta X^1_{\min}, \Delta X^2_{\min})$ of $\mathcal{G}^n$. We obtain V^{n+1} on $\mathcal{G}^n$.
- Step 2.1: Define $\mathcal{G}^{n+1,0} := \mathcal{G}^n$, and $V^{n+1,0} := V^{n+1}$ on $\mathcal{G}^n$.
- Step 2.2: For $1 \leq l \leq L_{\max} - 1$, for all cells $M_j \in \mathcal{G}^{n+1,l} \cap \mathcal{G}_l$, compare the value[1] $V_j^{n+1,l}$ on M_j with its neighboring values. If the values are different, then refine cell M_j, attribute to the daugther cells of M_j the same value $V_j^{n+1,l}$. This defines a new grid $\mathcal{G}^{n+1,l+1}$. Set $l = l + 1$, and go to Step 2.2.
  Otherwise, set $l = L_{max}$ and go to step 2.3.

[1] Recall that for every $M_j \in \mathcal{G}^{n+1,l} \cap \mathcal{G}_l$, with $\underline{l < L_{\max}}$, the mean value $V_j^{n+1,l}$ is equal to 0 or 1.

- Step 2.3: Set $\widetilde{\mathcal{G}}^{n+1,L_{\max}} := \mathcal{G}^{n+1,L_{\max}}$ and $\widetilde{V}^{n+1,L_{\max}} := V^{n+1,L_{\max}}$.
- Step 2.4: For $l = L_{\max}, \cdots, 2$, do a corsening step following the same idea as in Step 1.4. If there is no coarsening to do, then set $l = 1$, and go to Step 2.5.
- Step 2.5: Set $\mathcal{G}^{n+1} := \widetilde{\mathcal{G}}^{n+1,1}$, and $V^{n+1} := \widetilde{V}^{n+1,1}$. This corresponds to the approximation on $\mathcal{G}^{n+1}$ of the solution $\hat{v}$ of (12) at $t = t^{n+1}$.

By construction, we have the following equivalence result:

Theorem 1 *Let $L_{\max}$ be a fixed integer. Under the CFL condition (13), the approximation of (12) using the UB-HJB scheme on an adaptative grid gives the same numerical solution as the resolution using the UB-HJB scheme on a regular grid $\mathcal{G}_{L_{\max}}$.*

4 Numerical simulations

In the graphics through all this section, we use the black color for cells with mean value strictly between 0 and 1, white for cells with value 0 and light gray for cells with value 1. We also use the notation $\mathcal{B}(c_0, r)$ for the ball centered in c_0 and with radius r.

Example 1: A propagating front problem
We first start with a propagating fronts problem. The initial condition is here two sources from which a fire spreads. Let φ be a function that modelizes the burnt region at $t = 0$, and defined as :

$$\varphi(x) = \begin{cases} 0 & \text{if } x \in \mathcal{B}(c_1, 0.1) \cup \mathcal{B}(c_2, 0.1), \\ 1 & \text{otherwise,} \end{cases}$$

with $c_1 = (0.4, 0.4)$ and $c_2 = (0.6, 0.6)$. Let $\mathcal{K}$ denote the domain $[-0.5, 2.5] \times [-1.5, 1.5]$. We associate to this problem the function $\hat{v}$ which takes value 0 in $(t, x) \in [0, T] \times \mathcal{K}$ if the flame front has already reached x at t, and 1 otherwise. In fact, $\hat{v}$ satisfies the Eikonal equation,

$$\begin{cases} \hat{v}_t(t,x) + ||\nabla \hat{v}(t,x)|| + (-x_2, x_1)^t . \nabla \hat{v}(t,x) = 0, \ \forall t \in [0,T], \ \forall x = (x_1, x_2) \in \mathcal{K}, \\ \hat{v}(0,x) = \varphi(x), \ \forall x \in \mathcal{K}. \end{cases} \tag{14}$$

The discontinuity of $\hat{v}$ at time t is the position of the flame front at time t. Hence the set $\{x \in \mathcal{K}, \hat{v}(t,x) = 0\}$ represents the burnt zone at time t.
Although this problem comes from front propagation, it takes place in the formalism we study. Indeed, the Eikonal equation (14) can be written as an HJB equation:

$$\begin{cases} \hat{v}_t(t,x) - \min_{a \in \mathcal{A}} f(x,a) . \nabla \hat{v}(t,x) = 0, \ \forall t \in [0,T], \ \forall x \in \mathcal{K}, \\ \hat{v}(0,x) = \varphi(x), \ \forall x \in \mathcal{K}, \end{cases}$$

where the set of controls is $\mathcal{A} = [0, 2\pi]$, and the dynamics is given by:

$$f(x,a) = (x_2 - \cos(a), -x_1 - \sin(a))^t, \ \forall x \in \boldsymbol{R}^2, \ \forall a \in \mathcal{A}.$$

In the numerical tests, we discretize $\mathcal{A}$ into $N_a = 8$ controls, and we choose $L_{max} = 6$ as maximal level of refinement. We visualize the computed solution and the error which is defined on each cell M_j, for $j \in J$, by $\varepsilon_j^n = |V_j^n - \widetilde{V}_j^n|$. Here $\widetilde{V}_j^n$ is the average value of the exact solution $\hat{v}$ on cell M_j at time t^n.

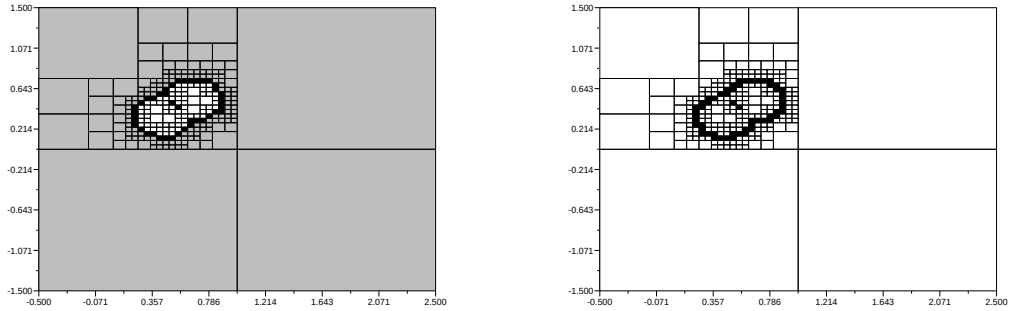

(a) computed solution (b) error $(\varepsilon_j^n)_{j\in J}$

Figure 3: Computed solution and error at T=0.11, # cells=244, $L_{max} = 6$.

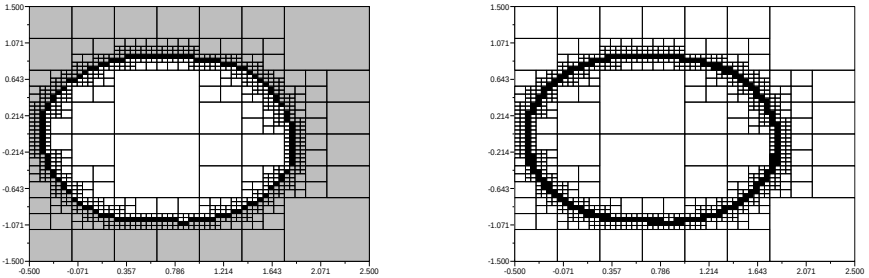

(a) computed solution (b) error $(\varepsilon_j^n)_{j\in J}$

Figure 4: Computed solution and error at T=0.87, # cells=817, $L_{max} = 6$.

We display graphics at $T = 0.11$ (figure 3) when the two fronts meet, and then at $T = 0.87$ (figure 4) when we get only one front which is already far from the sources of fire. Notice that the error is localized in a thin region around the discontinuity of bandwidth of no more than twice the size of a minimal cell. This is the antidissipative behavior of the scheme. Notice also that the approximation quality isn't distorted when the discontinuity evolves in time. This is another feature of the antidissipative behavior.

Grid	L_{max}	L^1 error	# cells	gain
adapt	6	8.8E-3	244	16.78
reg	6	8.8E-3	4096	-
adapt	7	5.67E-3	547	29.95
reg	7	5.67E-3	16384	-
adapt	8	4E-3	1108	59.14
reg	8	4E-3	65536	-
adapt	9	3E-3	1939	135.195
reg	9	3E-3	262144	-
adapt	10	2.46E-3	3940	266.14
reg	10	-	1048576	-

Table 1: Gain relative to each refinement level at T=0.11.

Table 1 summerizes the gain we obtain in terms of number of cells when we apply adaptation by comparison to an equivalent regular grid. We can notice that, as expected, we obtain exactly the same error on an adaptative grid and on a regular one. Notice that when we increase the refinement level by 1, the gain is multiplied by 2 and the error is multiplied by $\frac{2}{3}$. This reflects optimization in the management of cells. We can also notice at $T = 0.11$ that when we fix $L_{max} = 10$ we handle almost 4000 cells on an adaptative grid, as much cells as if we did calculations on a regular grid corresponding to $L_{max} = 6$. Hence when we adapt the grid we improve the precision 3 times without spending any additional memory cost. For refinement levels bigger than 10, it is no more possible to handle calculations on a regular grid. Hence we can not have better precision on a regular grid: this reflects the gain of precision achieved by the use of the adaptative algorithm.
For the moment we have only comparable CPU times for both methods, the reason is that the program for handling an adaptative meshing is not optimized, while an optimized version is used for the regular mesh computation. Improvement of the adaptative computation is in progress.

Example 2: A capture basin problem (Zermelo problem)
Let $\mathcal{K} := [-6, 2] \times [-2, 2]$ and $\mathcal{C} := \mathcal{B}(c_0, r)$ with $c_0 = (0, 0)$ and $r = 0.44$. We define the dynamics $f : \boldsymbol{R}^2 \times \mathcal{A} \to \boldsymbol{R}^2$,

$$f(x, a, \theta) = (1 - \beta x_2^2 + a\cos(\theta), a\sin(\theta)),$$

where the constant $\beta = 0.1$, and $\mathcal{A}$ denotes the set $[0, 0.44] \times [0, 2\pi[$.

Our aim is to approximate the capture basin of $\mathcal{C}$ which is the subset of initial states $x \in \mathcal{K}$ for which exists an admissible control $(a, \theta) \in L^\infty([0, +\infty[; \mathcal{A})$ and a finite time $t \geq 0$ such that the trajectory $y_{x,0}(.)$ evolving with the dynamics f under (a, θ) lives in $\mathcal{K}$ and reaches $\mathcal{C}$ at time t :

$$\text{Capt}_f(\mathcal{C}) := \{x \in \mathcal{K},\ \exists t \geq 0,\ \exists (a, \theta) \in L^\infty(\boldsymbol{R}^+; \mathcal{A}),\ y_{x,0}(\tau) \in \mathcal{K}\ \forall \tau \in [0, t],\ y_{x,0}(t) \in \mathcal{C}\}.$$

We consider the capture basin of $\mathcal{C}$ before time T:

$$\mathrm{Capt}_f(T,\mathcal{C}) := \{x \in \mathcal{K},\ \exists t \in [0,T],\ \exists (a,\theta) \in L^\infty([0,T];\mathcal{A}),\ y_{x,0}(.) \in \mathcal{K},\ y_{x,0}(t) \in \mathcal{C}\}.$$

It is clear that $T \mapsto \mathrm{Capt}_f(T,\mathcal{C})$ is increasing for inclusion. Moreover, we can prove [6] that $\lim_{T\to+\infty} \mathrm{Capt}_f(T,\mathcal{C}) = \mathrm{Capt}_f(\mathcal{C})$. Let us set

$$\varphi(x) = 0 \text{ if } x \in \mathcal{C}, \quad \text{and 1 otherwise,}$$

and consider the set-valued map defined by

$$\Lambda(x) = \begin{cases} 0 & \text{if } x \in \overset{\circ}{\mathcal{C}}, \\ [0,1] & \text{if } x \in \partial\mathcal{C}, \\ \{1\} & \text{if } x \in \mathcal{K} \setminus \mathcal{C}. \end{cases}$$

Let v_T be the value function of the following control problem:

$$\begin{array}{l} \min\{\varphi(y_{x,s}(T)), \\ \dot{y}_{x,s}(t) = \lambda(t) f(y_{x,s}(t), a(t), \theta(t)), \quad y_{x,s}(s) = x, \\ (a(t),\theta(t)) \in \mathcal{A} \quad \& \quad \lambda(t) \in \Lambda(y_{x,s}(t)) \quad \text{for a.e. } t \in (0,T), \\ y_{x,s}(t) \in \mathcal{K}\ \forall t \in [0,T]. \end{array}$$

We use the classical change of variable: $\hat{v}(t,x) = v_T(T-t,x),\ \forall t \in [0,T],\ \forall x \in \mathcal{K}$. Then, following [6], we have:

$$\mathrm{Capt}_f(T,\mathcal{C}) = \{x \in \mathcal{K},\ v_T(0,x) = 0\} = \{x \in \mathcal{K},\ \hat{v}(T,x) = 0\}.$$

Then as in [6], in order to approximate $\mathrm{Capt}_f(\mathcal{C})$, we compute an approximation V^n of $\hat{v}(t^n,\cdot)$, with $t^n := n\Delta t$, for n large enough and satisfying the stopping test

$$||V^n - V^{n-1}||_{L^1} := \sum_j \Delta x^1_{min} \Delta x^2_{min} |V^n_j - V^{n-1}_j| \le 10^{-4}. \tag{15}$$

In figure 5, we show the graphics we obtain for maximal level of refinement $L_{max} = 6$ (figure 5 (a)) and $L_{max} = 7$ (figure 5 (b)). In the graphics, the black circle is the border of the target $\mathcal{C}$. We give in the following table the gain obtained for each refinement level, the stopping time (i.e time for which the stopping test (15) is fulfilled) and the value of the residual $||V^n - V^{n-1}||_{L^1}$. Notice that when we increase the refinement level L_{max}, the precision required in the stopping test is reached faster. For example, with $L_{max} = 7$ we obtain a good solution on the adaptative grid at $T = 7.187$ using 952 cells, whereas with $L_{max} = 5$, the stopping test is fulfilled only after $T = 26.125$ and the corresponding regular grid contains 1024 cells. Hence adaptative gridding allows not only to have a better precision using almost the same number of cells but also to handle less calculations and to save time.

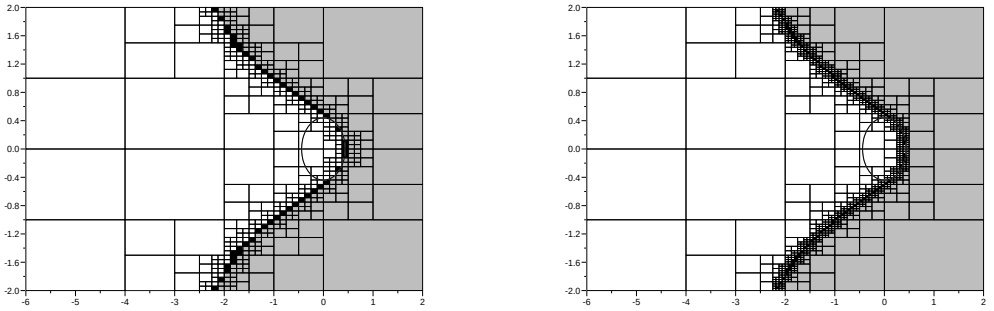

(a) L_{max}=6, $T = 12.96$, # cells=478 (b) L_{max}=7, $T = 7.18$, # cells=952

Figure 5: Capture basin of a Zermelo problem.

Grid	L_{max}	# cells	gain	stopping time	$\|\|V^n - V^{n-1}\|\|_{L^1}$
adapt	5	232	4.41	26.125	3.89 E-7
reg	5	1024	-	26.125	3.89 E-7
adapt	6	478	8.56	12.96	1.82 E-8
reg	6	4096	-	12.96	1.82 E-8
adapt	7	952	17.21	7.187	2.38 E-5
reg	7	16384	-	7.187	2.38 E-5

Table 2: Gain relative to each refinement level with the value of the residual and the stopping time.

Example3: A viability kernel problem (consumption problem)
Let $\mathcal{K} = [0,2] \times [0,3]$, $\mathcal{A} = [-\frac{1}{2}, \frac{1}{2}]$ and $f(x,a) = (x_1 - x_2, a)$, $\forall x \in \boldsymbol{R}^2$, $\forall a \in \mathcal{A}$.

We define the viability kernel associated to $\mathcal{K}$ as the set of initial states $x \in \mathcal{K}$ such that exists a control $a \in L^\infty(\boldsymbol{R}^+; \mathcal{A})$ and a trajectory $y_{x,0}(.)$ (evolving under the control a) which never leaves $\mathcal{K}$,

$$\text{Viab}(\mathcal{K}) := \{x \in \mathcal{K}, \exists a \in L^\infty(\boldsymbol{R}^+; \mathcal{A}),\ y_{x,0}(t) \in \mathcal{K}\ \forall t \geq 0\}.$$

We define also

$$\text{Viab}(T, \mathcal{K}) := \{x \in \mathcal{K}, \exists a \in L^\infty([0,T], \mathcal{A}),\ y_{x,0}(t) \in \mathcal{K}\ \forall t \in [0,T]\}.$$

Let $\varphi(x) = 0$ if $x \in \mathcal{K}$, and 1 otherwise. Consider the value function v_T of the control problem (1) associated to the dynamics f, the final cost φ and the set $\mathcal{K}$.

Let $\hat{v}(t,x) = v_T(T-t,x)$. From [6], we have: $\text{Viab}(T,\mathcal{K}) = \{x \in \mathcal{K},\ \hat{v}(T,x) = 0\}$, and $\text{Viab}(T,\mathcal{K}) \longrightarrow_{T \to +\infty} \text{Viab}(\mathcal{K})$. As in the previous example, in order to approximate $\text{Viab}(\mathcal{K})$, we compute an approximation V^n of $\hat{v}(t^n, \cdot)$ for n satisfying the same stopping test (15).

We show the graphics we obtain for maximal level $L_{max} = 5$ (figure 6 (a)) and $L_{max} = 6$ (figure 6 (b)). In these figures, the white line is the border of the exact viability kernel. Here, the set of controls $\mathcal{A}$ is discretized into $N_a = 2$ controls ($a \in \{-\frac{1}{2}, \frac{1}{2}\}$).

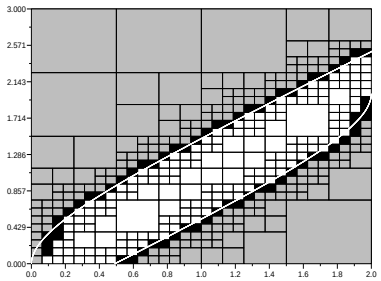

(a)L_{max}=5, $T \approx 256$, # cells=421

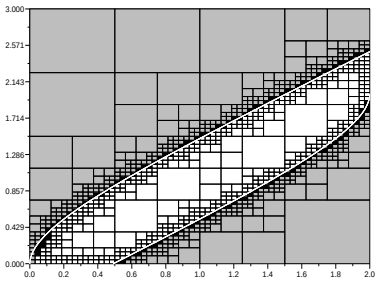

(b)L_{max}=6, $T \approx 5$, # cells=916

Figure 6: Viability kernel of the consumption problem.

In a previous work [6], the UB-HJB scheme has been compared to the viability algorithm [21]. Many numerical examples have been handled on a regular grid (among others the Zermelo problem and the consumption problem) to prove the relevance of UB-HJB in this kind of problems. In fact, UB-HJB provides a much better approximation of these sets (viability kernels, capture basins). Here we continue in the same direction and improve results given by UB-HJB scheme. The use of the adaptative method allows us to reach a better precision by optimizing the management of the memory.

5 Appendix: Generalized solutions of the HJB equation

The aim of this appendix is to give a global view of the different notions of solution of the HJB equation. Especially to summarize some results concerning the characterization of the value function v as the unique solution (in a sense that has to be explicited) of this equation. The sense of solution depends essentially on the regularity of the final cost function φ and on the set $\mathcal{K}$. We recall that we keep the assumptions of the introduction on the dynamics f and the set of controls $\mathcal{A}$. We define the Hamiltonian

$$\mathcal{H}(x,p) = -\min_{a\in\mathcal{A}} f(x,a).p,\ \forall (x,p)\in \mathcal{K}\times \boldsymbol{R}^n.$$

The case when $\mathcal{K} = \boldsymbol{R}^n$. The first result of characterization of the value function was given in the pioneering works of Crandall, Evans and Lions [9, 10] in the case when φ is bounded continuous and $\mathcal{K} = \boldsymbol{R}^n$. In fact they proved that v is the unique bounded *continuous viscosity* solution of the HJB equation:

$$-v_t(t,x) + \mathcal{H}(x, v_x(t,x)) = 0, \qquad (t,x)\in]0,T[\times\mathcal{K}, \tag{16}$$

satisfying $v(T,x) = \varphi(x),\ \forall x\in\mathcal{K}$. For the convenience of the reader, we recall here the definition of the viscosity notion:

Definition 1 *i) u upper semi continuous (u.s.c) on $[0,T]\times\mathcal{K}$ is a viscosity sub-solution of (16) if it satisfies for all $\phi\in\mathcal{C}^1([0,T]\times\mathcal{K})$, for all (t_0,x_0) local maximum on $]0,T[\times\mathcal{K}$ of $u-\phi$,*

$$-\phi_t(t_0,x_0) + \mathcal{H}(x_0,\phi_x(t_0,x_0)) \le 0.$$

ii) u lower semi continuous (l.s.c) on $[0,T]\times\mathcal{K}$ is a viscosity super-solution of (16) if it satisfies for all $\phi\in\mathcal{C}^1([0,T]\times\mathcal{K})$, for all (t_0,x_0) local minimum on $]0,T[\times\mathcal{K}$ of $u-\phi$,

$$-\phi_t(t_0,x_0) + \mathcal{H}(x_0,\phi_x(t_0,x_0)) \ge 0.$$

iii) u continuous on $[0,T]\times\mathcal{K}$ is a viscosity solution of (16) if it is a viscosity super-solution and a viscosity sub-solution of (16).

Now, let $(t_0,x_0)\in(0,T)\times\mathcal{K}$, and consider the sub-differential D^-u and the super-differential D^+u of u given by:

$$D^+u(t_0,x_0) := \left\{ p\in\boldsymbol{R}^{n+1},\ \limsup_{\substack{(t,x)\to(t_0,x_0)\\(t,x)\in[0,T]\times\mathcal{K}}} \frac{u(t,x)-u(t_0,x_0)-p.(t-t_0,x-x_0)}{|(t-t_0,x-x_0)|} \le 0 \right\},$$

$$D^-u(t_0,x_0) := \left\{ p\in\boldsymbol{R}^{n+1},\ \liminf_{\substack{(t,x)\to(t_0,x_0)\\(t,x)\in[0,T]\times\mathcal{K}}} \frac{u(t,x)-u(t_0,x_0)-p.(t-t_0,x-x_0)}{|(t-t_0,x-x_0)|} \ge 0 \right\}.$$

Using these sets, the notion of viscosity solution can be defined equivalently as follows:
i) u u.s.c is a viscosity sub-solution of (16) iff:

$$\forall (t,x) \in]0,T[\times\mathcal{K},\ \forall (p_t,p_x) \in D^+u(t,x),\ -p_t + \mathcal{H}(x,p_x) \leq 0.$$

ii) u l.s.c is a viscosity super-solution iff:

$$\forall (t,x) \in]0,T[\times\mathcal{K},\ \forall (p_t,p_x) \in D^-u(t,x),\ -p_t + \mathcal{H}(x,p_x) \geq 0.$$

Let us mention that if u is a differentiable classic solution of the HJB equation then it is a viscosity solution of the equation. Conversely, a continuously differentiable viscosity solution is a classic solution of the HJB equation.

Thanks to the convexity of the Hamiltonian $\mathcal{H}(x,.)$, Barron and Jensen [3] proved that a continuous function u is a viscosity solution of (16) if it satisfies equivalently

$$\forall (t,x) \in]0,T[\times\mathcal{K},\ \forall (p_t,p_x) \in D^-u(t,x),\ -p_t + \mathcal{H}(x,p_x) = 0. \tag{17}$$

Hence, contrary to the definition of Crandall and Lions, we need to "touch" the solution by test functions only from below.

As the definition of Barron and Jensen uses only the l.s.c character of the function, we can extend it to l.s.c functions.

Definition 2 *A l.s.c function satisfying (17) is called a l.s.c viscosity solution of the HJB equation.*

With the above definition, Barron and Jensen [3, 4] proved that when φ is l.s.c and $\mathcal{K} = \boldsymbol{R}^n$, then the l.s.c envelope v_* of the value function:

$$v_*(t,x) = \liminf_{(t',x')\to(t,x)} v(t',x'),$$

is the unique l.s.c viscosity solution of the HJB equation (16) satisfying the final condition

$$\liminf_{(t',x')\to(T,x)} v_*(t',x') = \varphi(x),\ \forall x \in \boldsymbol{R}^n. \tag{18}$$

On the other hand, under the following additional convexity hypothesis:

$$\mathcal{A} \text{ is convex,} \quad \text{and } \{f(x,a),\ a \in \mathcal{A}\} \text{ is convex } \forall x \in \boldsymbol{R}^n, \tag{19}$$

Frankowska proved in [14] that the value function is the unique l.s.c solution of the HJB equation (16) satisfying the final condition (18).

When $\mathcal{K}$ is a compact of $\boldsymbol{R}^n$. Now when the set $\mathcal{K}$ is a compact of $\boldsymbol{R}^n$ and the final cost φ is continuous, the value function may be discontinuous. As $\mathcal{K}$ is no more an open set but a closed set, the notion of viscosity has to be handled with some care. In fact, if u is a viscosity super-solution of (16) on an open set Ω, this doesn't imply that u is a super-solution of (16)

on a closed set $\overline{\Omega'} \subset \Omega$.

Under the inward pointing qualification constraint introduced by Soner [23]:

$$\exists \nu > 0,\ \forall x \in \partial\mathcal{K},\ \exists a \in \mathcal{A},\ f(x,a).\eta(x) \leq -\nu, \tag{IP}$$

(here η is the outward normal to $\mathcal{K}$ and $\partial\mathcal{K}$ is regular) the value function is proved to be continuous and is characterized as the unique *constrained viscosity* solution of the HJB equation (16), in the following sense:

Definition 3 *A bounded function is a constrained viscosity solution of* (16) *iff it is a viscosity sub-solution on* $]0,T[\times \overset{\circ}{\mathcal{K}}$ *and a viscosity super-solution on* $]0,T[\times\mathcal{K}$.

An extension of this work is given by Ishii and Koike [20] under the following weaker qualification constraint:

$$\mathcal{A}(x) \neq \emptyset,\ \ \forall x \in \partial\mathcal{K}, \tag{VC}$$

with $\mathcal{A}(x) = \{a \in \mathcal{A},\ \exists r > 0,\ y_{\xi,0}(t) \in \mathcal{K}\ \forall \xi \in \mathcal{B}(x,r) \cap \mathcal{K},\ t \in [0,r]\}$. Let us first define the u.s.c envelope u^* and l.s.c envelpe u_* of a real valued function u:

$$\forall (t,x),\ u^*(t,x) = \limsup_{(t',x') \to (t,x)} u(t',x'),$$

$$\forall (t,x),\ u_*(t,x) = \liminf_{(t',x') \to (t,x)} u(t',x').$$

We also define the inward Hamiltonian :

$$\mathcal{H}_{in}(x,p) = -\min_{a \in \mathcal{A}(x)} f(x,a).p,\ \forall (x,p) \in \mathcal{K} \times \boldsymbol{R}^n.$$

The result of [20] says that, under the qualification constraint (VC), v is a discontinuous viscosity solution of (16), in the following sense.

Definition 4 *A bounded function u is a discontinuous viscosity solution of the HJB equation (16) if it satisfies*

$$-(u^*)_t(t,x) + \mathcal{H}_{in}(t,x,(u^*)_x(t,x)) \leq 0\ \forall (t,x) \in]0,T[\times\mathcal{K},$$

and

$$-(u_*)_t(t,x) + \mathcal{H}(x,(u_*)_x(t,x)) \geq 0\ \forall (t,x) \in]0,T[\times\mathcal{K},$$

in the viscosity sense.

We remark that the constraint (VC) means that there exists a viable trajectory $y_{x,0}(.)$ for each starting point $x \in \mathcal{K}$. Viability means that $y_{x,0}(.)$ keeps in $\mathcal{K}$ all the time. Whereas the inward pointing qualification constraint (IP) insures the existence of a trajectory which remains in the interior of $\mathcal{K}$.

Under another qualification constraint called outward pointing:

$$\forall x \in \partial\mathcal{K},\ \exists a \in \mathcal{A},\ f(x,a).\eta(x) > 0, \tag{OP}$$

Frankowska et al. [15, 16, 17] studied the case when $\mathcal{K}$ is a compact set with a regular border and eventually an empty interior, and φ is proper and l.s.c. In this case, if the convexity assumption (19) holds, then the value function v is characterized as the unique l.s.c solution of the HJB equation, in the sense that it satisfies:

$$\begin{aligned}
&\liminf_{\substack{(t_n,x_n)\to(T^-,x)\\ x_n\in\overset{\circ}{\mathcal{K}}}} v(t_n,x_n) = \varphi(x), \quad \forall x \in \mathcal{K},\\
&\liminf_{\substack{(t_n,x_n)\to(0^+,x)\\ x_n\in\mathcal{K}}} v(t_n,x_n) = v(0,x), \quad \forall x \in \mathcal{K},\\
&-p_t + \mathcal{H}(x,p_x) \geq 0, \quad \forall (p_t,p_x) \in D^- v(t,x),\ \forall (t,x) \in]0,T[\times\partial\mathcal{K},\\
&-p_t + \mathcal{H}(x,p_x) = 0, \quad \forall (p_t,p_x) \in D^- v(t,x),\ \forall (t,x) \in]0,T[\times \overset{\circ}{\mathcal{K}}.
\end{aligned}$$

The outward pointing qualification (OP) means the existence of a control variable which allows to leave $\mathcal{K}$, but not tangentially to the border $\partial\mathcal{K}$.

References

[1] M. Bardi and I. Capuzzo-Dolcetta, *Optimal control and viscosity solutions of Hamilton-Jacobi-Bellman equations*, Systems and Control: Foundations and Applications.Birkhäuser, Boston, 1997.

[2] G. Barles, *Solutions de viscosité des équations de Hamilton-Jacobi.* Mathématiques et applications. Springer, Paris,17, 1994.

[3] E. N. Barron and R. Jensen, *Semicontinuous viscosity solutions for Hamilton-Jacobi equations with convex Hamiltonian.* Comm. Partial Differential equations 15 (1990), 1713-1742.

[4] E. N. Barron and R. Jensen, *Optimal control and semi-continuous viscosity solutions.* Proc. Amer. Math. Soc. 113 (1991) n°2 397-402.

[5] O. Bokanowski and H. Zidani, *Anti-dissipative schemes for advection and application to Hamilton-Jacobi-Bellmann equations.* Preprint, INRIA Report RR-5337, 2004.

[6] O. Bokanowski, S. Martin, R. Munos and H. Zidani, *An Anti-diffusive scheme for viability problems.* INRIA Report RR-5431, 2004.

[7] O. Bokanowski, N. Megdich and H. Zidani, *On the convergence of a non-monotone scheme for HJB equations.* in preparation.

[8] I. Capuzzo-Dolcetta and P. L. Lions, *Hamilton-Jacobi equations with state constraints.* Transactions of the american mathematical society, vol 318, p 643-685, 1990.

[9] M. G. Crandall and P. L. Lions, *Viscosity solutions of Hamilton-Jacobi equations.* Transactions of the american mathematical society, vol 277, p 1-42, 1983.

[10] M. G. Crandall, L. C. Evans and P. L. Lions, *Some properties of viscosity solutions of Hamilton Jacobi equations.* Tran. Amer. Math. Soc. Vol 282 n°2,(1984).

[11] B. Després and F. Lagoutière, *Contact discontinuity capturing schemes for linear advection and compressible gas dynamics.* J.Sci. Comput. 16(2001), 479-524.

[12] M. Falcone and R. Ferretti, *Semi-Lagrangian schemes for Hamilton-Jacobi equations, discrete representation formulae and Godunov methods.* Journal of computational physics, 175:559-575, 2002.

[13] M. Falcone and T. Giorgi, *An approximation scheme for Evolutive Hamilton-Jacobi Equations.* Dipartemento di Matematica , Università di Roma "La Sapienza", preprint 1994.

[14] H. Frankowska *Lower semi-continuous solutions of Hamilton-Jacobi-equations.* SIAM J.Control Optim. 31 (1993), 257-272.

[15] H. Frankowska and S. Plaskacz, *Semicontinuous solutions of Hamilton-Jacobi equations with state constraints.* Differential inclusions and optimal control, Lecture notes in nonlinear analysis, J.Schauder center for nonlinear studies, edited by J.Andres, L.Gorniewicz, P.Nastri, Vol 2, 145-161, (1998).

[16] H. Frankowska and R. B. Vinter, *Existence of neighboring feasible trajectories: applications to dynamic programming for state-constraint optimal control problems.* Journal of optimization theory and applications. Vol 104(2000),27-40.

[17] H. Frankowska and S. Plaskacz, *Semicontinuous solutions of Hamilton-Jacobi-Bellman equations with degenerate state constraints.* JMAA. Vol 251(2000),818-838.

[18] I. Gargantini, *An effective way to represent quadtrees.* Communications of the ACM, 25-12(1982), 905-910.

[19] L. Grune, *Adaptative grid generation for evolutive Hamilton-Jacobi-Bellman equations.* Numerical methods for viscosity solutions and applications, World scientific, 2001, 153-172.

[20] H. Ishii and S. Koike, *A new formulation of state constraint problems for first order PDES.* SIAM J. Control and Optimization, vol 34, n 2, (1996), 554-571.

[21] P. Saint-Pierre, *Approximation of viability kernel.* Appl.Math.Optim., 29, 187-209, 1994.

[22] P. E. Souganidis, *Approximation schemes for viscosity solutions of Hamilton-Jacobi equations.* Journal of differential equations, 59, 1-43, 1985.

[23] H. M. Soner, *Optimal control with state space constraint.* SIAM Journal of Control and Optimization, Vol 24, No 3, p 552-561, 1986.

Unité de recherche INRIA Rocquencourt
Domaine de Voluceau - Rocquencourt - BP 105 - 78153 Le Chesnay Cedex (France)

Unité de recherche INRIA Futurs : Parc Club Orsay Université - ZAC des Vignes
4, rue Jacques Monod - 91893 ORSAY Cedex (France)
Unité de recherche INRIA Lorraine : LORIA, Technopôle de Nancy-Brabois - Campus scientifique
615, rue du Jardin Botanique - BP 101 - 54602 Villers-lès-Nancy Cedex (France)
Unité de recherche INRIA Rennes : IRISA, Campus universitaire de Beaulieu - 35042 Rennes Cedex (France)
Unité de recherche INRIA Rhône-Alpes : 655, avenue de l'Europe - 38334 Montbonnot Saint-Ismier (France)
Unité de recherche INRIA Sophia Antipolis : 2004, route des Lucioles - BP 93 - 06902 Sophia Antipolis Cedex (France)

Éditeur
INRIA - Domaine de Voluceau - Rocquencourt, BP 105 - 78153 Le Chesnay Cedex (France)
http://www.inria.fr
ISSN 0249-6399